Lowest Optical Excitations in Molecular Crystals: Bound Excitons versus Free Electron-Hole Pairs in Anthracene

Kerstin Hummer,[1] Peter Puschnig,[1,2] and Claudia Ambrosch-Draxl[1]

[1]*Institut für Theoretische Physik, Karl-Franzens Universität Graz, Universitätsplatz 5, 8010 Graz, Austria*
[2]*Institut für Wärmetechnik, Technische Universität Graz, Inffeldgasse 25/B, 8010 Graz, Austria*

(Received 10 September 2003; published 8 April 2004)

By solving the Bethe-Salpeter equation for the electron-hole Green function for crystalline anthracene we find the lowest absorption peak generated by strongly bound excitons or by a free electron-hole pair, depending on the polarization direction being parallel to the short or the long molecular axis, respectively. Both excitations are shifted to lower energies by pressure. The physical difference of these excitations is apparent from the electron-hole wave functions. Our findings are a major contribution to solve the long-standing puzzle about the nature of the lowest optical excitations in organic materials.

DOI: 10.1103/PhysRevLett.92.147402 PACS numbers: 78.40.Me, 71.15.Mb, 71.35.Cc

Organic materials consisting of small π-conjugated molecules experience their renaissance in *plastic electronics* research. For more than two decades this research field has concentrated on organic polymers. Doped polyacetylene (PA) [1,2], poly(*para*-phenylene) [3,4], and poly(*para*-phenylene vinylene (PPV) [5] have been among the most prominent polymers of interest. The device characteristics of a variety of such materials have been investigated, and the technological applicability in organic field effect transistors or organic light emitting diodes has been realized for many of them [6,7]. Studies on the optical absorption processes in organic polymers give controversial answers to the question, whether the lowest energy transition is due to free charge carriers (direct interband transitions) or the absorption of tightly bound excitons (Frenkel exciton model) [8,9]. In this context the experimentally determined exciton binding energy published for PPV ranges from 0.1 to 0.9 eV [10].

The optoelectronic properties strongly depend on the crystalline structure of such materials, which in turn is governed by the intermolecular (interchain) interactions inherently present in the three-dimensional (3D) environment. The importance of considering these interactions in theoretical models to correctly describe organic semiconductors properties has been pointed out recently [11,12]. Highly reliable *ab initio* methods allowed one to attain understanding of the mechanism involved in their photophysics and to clarify the importance of these interactions on the material-dependent electro-optical activity. For example, in PA, *ab initio* calculations considering the full crystal symmetry have shown that, compared to the isolated PA chain, the exciton wave function is distributed even to neighboring chains and thus the exciton binding energy is reduced by an order of magnitude [12].

In contrast to organic polymers, where the building blocks are *infinite* chains, oligomers [13,14] built by finite molecules form well defined crystals. In particular, oligophenylenes [15,16], oligothiophenes [17,18], as well as pentacene [19,20] are promising candidates for electro-optical devices. It is commonly believed that the intermolecular interactions in organic molecular crystals are weak, and therefore the electron-hole (*e-h*) pairs are basically confined to single molecules resulting in large exciton binding energies. For anthracene, which is a prime example for organic molecular crystals, it was found that its photophysics is determined by tightly bound excitons and that the molecular exciton theory [21] is able to correctly describe the lowest optical absorption processes [13,22]. However, the Bethe-Salpeter equation (BSE) has hardly been performed for molecular crystals.

In this Letter, we address the questions how large the exciton binding energy in crystalline anthracene is and how it depends on the intermolecular interactions. These interactions can be altered in a controlled way by applying hydrostatic pressure. Starting with the experimentally observed lattice parameters under pressure [23], the molecular and internal geometry of anthracene have been optimized [24] utilizing the full-potential augmented plane wave plus local orbitals method [25] as implemented in the WIEN2K code [26]. Based on these structures, the electronic band structures [24] and the dielectric tensors within the random phase approximation (RPA) have been calculated. An increase of band dispersion and band splitting has been obtained, resulting in a band gap reduction and consequently a redshift and broadening of the optical absorption peaks [27]. In this work, we calculate for the first time the dielectric tensor including *e-h* interaction by solving the BSE for the *e-h* two-particle Green function [28,29] for anthracene. A detailed description of this formalism and its implementation in the linearized augmented plane wave method is given in Ref. [30]. The WIEN2K specific parameters, those connected to the BSE formalism used for all calculations, and convergence tests for anthracene will be published elsewhere [31]. Regarding the computational

 © 2004 The American Physical Society

methods underlying the results presented herein, we point out that the statically screened Coulomb interaction $W(\mathbf{r}, \mathbf{r}')$ entering the two-particle Hamiltonian is obtained in terms of the full inverse dielectric matrix according to Eq. (13) in Ref. [30]. Note that vibronic splitting is not included in our theoretical approach, and, therefore, line shapes cannot be compared to the experimentally observed ones.

Let us now address the excitonic effects in anthracene. In Fig. 1 the two major components of the imaginary part of the dielectric tensor (DT) calculated within the RPA and by solving the BSE, respectively, are presented as a function of pressure. For consistency, the RPA and the BSE optical spectra have been corrected by a pressure dependent self-energy correction $\Delta_c(p)$, which will be discussed later. According to the monoclinic symmetry of the crystal, the computed DT consists of the Cartesian diagonal elements $\mathrm{Im}\varepsilon_{zz}$, $\mathrm{Im}\varepsilon_{yy}$, and $\mathrm{Im}\varepsilon_{xx}$, and the additional off-diagonal xz component. The Cartesian axes y and z are equivalent to the crystalline b and c axes, while the a axis deviates from x by the monoclinic angle β. Note that $\mathrm{Im}\varepsilon_{bb}$ ($\mathrm{Im}\varepsilon_{cc}$) corresponds to the optical response generated by light with the electric field vector almost parallel to the short (long) molecular axis, which is denoted with b (c, dashed line) in the inset of Fig. 1. The a component is minor and for this reason not displayed in Fig. 1. Both the RPA and the BSE find the lowest optical transition to be short-axis polarized and of weak oscillator strength. The inclusion of e-h interactions further identifies it as a strongly bound singlet exciton (S) below the RPA gap at 3.11 eV. The corresponding spin triplet exciton (T) is found further below in energy at 1.89 eV. The resulting singlet-triplet (S-T) splitting is 1.22 eV at ambient pressure, which perfectly reproduces

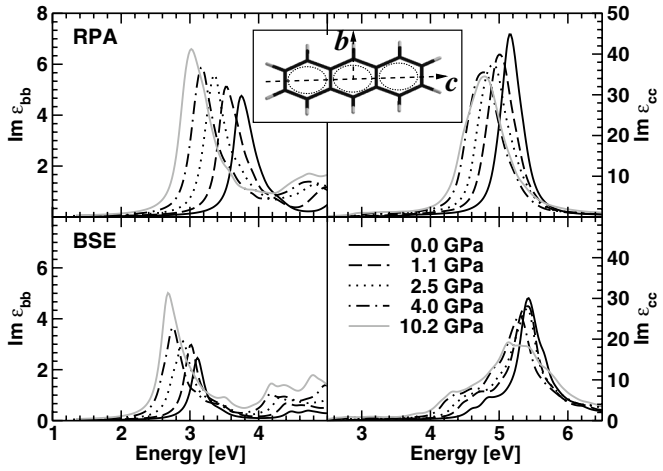

FIG. 1. b (c) component of the imaginary part of the DT on the left (right) calculated using the RPA (upper panels) compared to the solution of the BSE (lower panels) versus pressure. The spectra have been corrected by the self-energy Δ_c given in Table I. A lifetime broadening of 0.1 eV has been included. The inset shows one anthracene molecule, where the short (long) molecular axis is denoted by b (c).

the experimental value of 1.27 eV [13]. The spin singlet exciton binding energy (SBE), which is defined as the energy difference of the quasiparticle gap (RPA peak) and the S peak maximum, is 0.64 eV. This value is in good agreement with the experimental one of 0.8 eV, which has been deduced from measurements of the single-particle energy gap (3.9 ± 0.1 eV) [13]. As expected, it is larger compared to the values so far calculated for polymers [11,12], where such a high SBE has been obtained only for isolated polymer chains. Analogously to SBE, the triplet exciton binding energy (TBE) is determined to be 1.86 eV. If pressure is applied, S is shifted to lower energies (redshift) by approximately 0.4 eV up to 10.2 GPa. This pressure induced redshift is less pronounced than that suggested by the RPA. As a consequence, the SBE decreases with pressure and is reduced to almost 50% (0.34 eV) at 10.2 GPa (see Table II). In contrast to S, T is shifted to higher energies by pressure. Therefore, the TBE and the S-T splitting decrease with pressure, i.e., almost 50% at 10.2 GPa (Table II).

Now we concentrate on the response to c polarized light (right panels in Fig. 1). In this channel, an excitation with much larger oscillator strength is found. This is the second optically active absorption and in contrast to S, it appears above its corresponding RPA peak, indicating that it is due to a free e-h pair (FE). This long-axis polarized excitation is shifted to the red by pressure, but only half the amount of S, which is 0.2 eV up to 10.2 GPa. Again, the shift obtained by the BSE calculation is less pronounced than that observed within the RPA. The calculated c polarized absorption spectrum cannot be directly compared to experiment. However, the information about the c component is contained in the optical absorption measured with light polarized perpendicular to b, i.e., in the ac plane. Therefore, we can assign [33] the peaks in the measured photocurrent and extinction coefficient at 5.4–5.5 eV [14,34] at ambient pressure as a response to c polarized light. The agreement with our absorption peak at 5.4 eV is excellent. Also, the earlier published pressure experiments [32,35,36] have investigated only the b axis polarized spectrum and some perpendicular polarization direction. The performance of optical absorption measurements with light polarized along the crystalline c axis would be highly desirable, in

TABLE I. Calculated and experimentally observed optical energy gaps, E_g^{LDA} and E_g^{exp} [32], respectively, the resulting self-energy correction Δ_c, and the ratio between E_g^{LDA} and E_g^{exp} as a function of pressure.

p [GPa]	E_g^{LDA} [eV]	E_g^{exp} [eV]	Δ_c [eV]	$E_g^{\mathrm{LDA}} : E_g^{\mathrm{exp}}$
0.0	1.48	3.11	1.63	0.48
1.1	1.52	3.02	1.50	0.50
2.5	1.48	2.90	1.42	0.51
4.0	1.46	2.76	1.30	0.53
10.2	1.34	2.68		

TABLE II. The spin singlet (triplet) exciton binding energy SBE (TBE) and the singlet-triplet (S-T) splitting as a function of pressure.

p [GPa]	0.0	1.1	2.5	4.0	10.2
SBE [eV]	0.64	0.50	0.46	0.42	0.34
TBE [eV]	1.86	1.58	1.44	1.32	1.02
S-T [eV]	1.22	1.08	0.98	0.90	0.68

order to experimentally verify the big differences in the oscillator strengths of the components.

In order to further highlight the physical origin of the differences between the two optical excitations, as well as their pressure dependence, we have computed the excitonic wave functions according to $\Phi^{\lambda}(\mathbf{r}_e, \mathbf{r}_h) = \sum_{vc\mathbf{k}} A^{\lambda}_{vc\mathbf{k}} \psi^{*}_{v\mathbf{k}}(\mathbf{r}_h)\psi_{c\mathbf{k}}(\mathbf{r}_e)$. Therein $\mathbf{r}_e$ and $\mathbf{r}_h$ denote the electron and hole coordinates, respectively, whereas $\psi_{v\mathbf{k}}$ and $\psi_{c\mathbf{k}}$ are the single-particle wave functions for valence and conduction states with momentum $\mathbf{k}$. The coupling coefficients $A^{\lambda}_{vc\mathbf{k}}$ represent the eigenvectors of the effective e-h Hamiltonian. In Fig. 2 the electron distribution with respect to the hole at a fixed position calculated at ambient pressure on a rectangular 2D-grid including 4×4 unit cells is displayed for the ab plane (upper panels) and the ac plane (lower panels), respectively. The herringbone stacking of the molecules is clearly visible in the ab map of S, whereas the layered structure along c can be identified in the ac maps. In Fig. 3 the analogous electron distribution maps at 10.2 GPa are depicted. Let us focus on S at ambient pressure first (left panels in Fig. 2). There is no doubt that the electron of the e-h pair (dark regions) spreads over neighboring molecules along the a axis, but predominantly in the b direction. In the c direction, it is basically restricted to one unit cell, which explains the rather large SBE despite its extension in the ab plane. Now we compare the electron distribution of S with that of FE (right panels in Fig. 2). In case of S, the electron is found predominantly close to the hole. In contrast, the electron in FE avoids the vicinity of the hole, and thus it is not bound to it. This holds for both maps, the ab and ac plane, emphasizing the bound nature of S and the independency of the charge carriers in FE. Moreover, the FE is spread out to neighboring molecules in the ac plane to a higher extent than S. If pressure is applied, the extension of S in the ab plane is highly increased, whereas the e-h wave function remains rather confined in the c direction (bottom left panel in Fig. 2). While the former is the reason for the significant reduction of SBE with pressure, the latter ensures that the electron and the hole are still bound. As expected, pressure affects the electron distribution in FE to a smaller extent. In the ab map of FE we can see that the electron is now almost uniformly distributed with respect to the hole. From the comparison of the

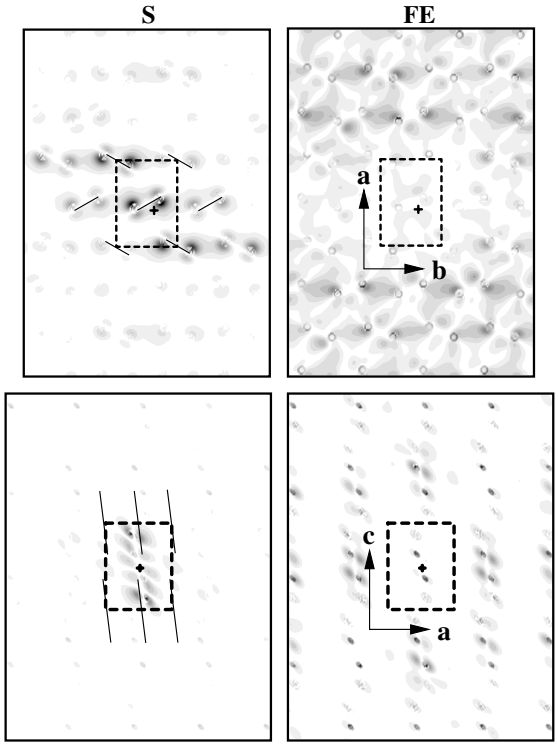

FIG. 2. The 2D electron distribution $|\psi_{c\mathbf{k}}(\mathbf{r}_e)|$ with respect to the hole at a fixed position (dark cross) calculated at ambient pressure for S (left) and FE (right), respectively. The unit cell is indicated by dashed rectangles and the molecules therein by thin solid lines. These ab (ac) maps represent slices at $z = 0.3$ ($y = 0.3$) with the hole located at $z = 0$ ($y = 0$) in units of c (b). The dark regions correspond to high density.

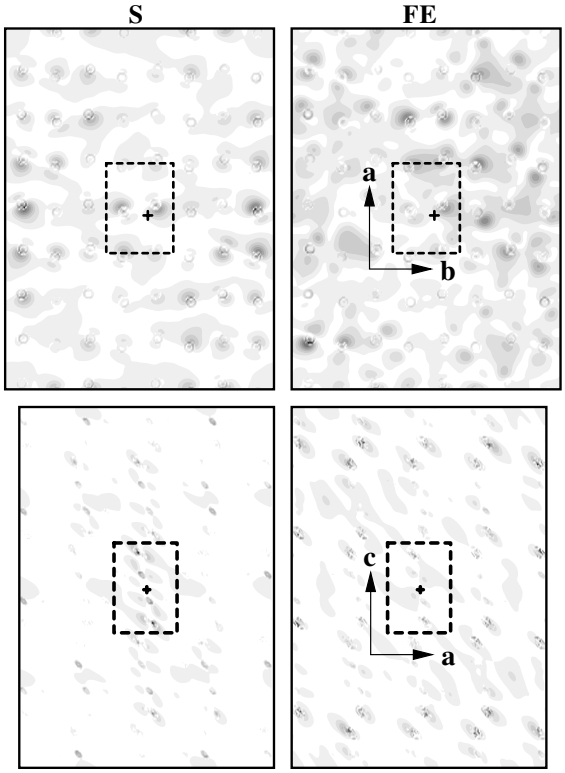

FIG. 3. Analogous to Fig. 2, but evaluated at 10.2 GPa.

FE *ac* maps at 0 and 10.2 GPa it is clear that the *e-h* wave function expands in the *a* direction by pressure. These observations are consistent with the pressure effect on the band structure and can be explained by the enhancement of the intermolecular interactions by pressure. These interactions are generally responsible for an increased dielectric screening and thus for the reduction of the *e-h* pair binding energy. Because of the anisotropy of this enhancement the redshift of FE is smaller compared to S.

Finally, we emphasize that all calculations of the imaginary part of the DT including *e-h* interactions have been performed without invoking the GW approach [37], which would provide the self-energy for correcting the gap calculated within the local density approximation (LDA). The comparison of the calculated optical gaps, E_g^{LDA}, to the experimentally observed ones, E_g^{exp} [32], up to 4 GPa allows us to determine the pressure dependence of the self-energy correction Δ_c. In Table I, E_g^{LDA}, E_g^{exp}, the resulting Δ_c, and the ratio between the theoretical and the experimental optical gaps are listed up to 10.2 GPa. The experimental error evaluated by comparison of two data sets [32,36] does not exceed 0.05 eV. Besides, the theoretical accuracy depends on the **k** mesh used for the calculation. The comparison to previous highly accurate RPA calculations makes us confident that the theoretical error is less than 0.1 eV. Regardless of these small uncertainties, the ratio between the theoretical and the experimental optical gaps up to 4 GPa is found to be a constant factor of approximately 0.5 independent of pressure. At this point we emphasize that the previously found underestimation of the LDA gap in various polymers by 40% [38] is true only within the RPA. We assume that this factor is still valid for higher pressures, which enables us to predict an optical gap of 2.68 ± 0.1 eV for 10.2 GPa. Moreover, this knowledge allows one to estimate the optical gap of other molecular crystals without performing the exact, but expensive, GW calculations for the self-energy correction.

In summary, our calculations clearly demonstrate that in one material, depending on the polarization of the probing light with respect to the crystalline axes, the physics underlying the optical response is different: We find a bound *e-h* pair with 0.64 eV binding energy as well as an excitation higher in energy, which can be traced back to free charge carriers. This fact is an important contribution to the ongoing discussion whether optical absorption processes in such materials are due to bound excitons or free electron-hole pairs. In general, absorption measurements for well defined polarization directions could further help to clarify the situation in different materials.

This work is supported by the Austrian Science Fund (Projects No. P14237 and No. P16227) and the EU RT network *EXCITING*, Contract No. HPRN-CT-2002-00317.

[1] H. Shirakawa *et al.*, J. Chem. Soc. Chem. Commun. No. 16, 578 (1977).
[2] C. K. Chiang *et al.*, Phys. Rev. Lett. **39**, 1098 (1977).
[3] D. M. Ivory *et al.*, J. Chem. Phys. **71**, 1506 (1979).
[4] G. Grem *et al.*, Adv. Mater. **4**, 36 (1992).
[5] J. H. Burroughes *et al.*, Nature (London) **347**, 539 (1990).
[6] A. J. Heeger, Synth. Met. **125**, 23 (2002).
[7] R. Friend *et al.*, Nature (London) **397**, 121 (1999).
[8] D. Moses *et al.*, Chem. Phys. Lett. **350**, 531 (2001).
[9] Z. Shuai *et al.*, Phys. Rev. Lett. **84**, 131 (2000).
[10] D. Moses *et al.*, Synth. Met. **125**, 93 (2002).
[11] A. Ruini *et al.*, Phys. Rev. Lett. **88**, 206403 (2002).
[12] P. Puschnig and C. Ambrosch-Draxl, Phys. Rev. Lett. **89**, 056405 (2002).
[13] E. A. Silinsh, *Organic Molecular Crystals* (Springer-Verlag, Berlin, Heidelberg, New York, 1980).
[14] M. Pope and C. E. Swenberg, *Electronic Processes in Organic Crystals and Polymers* (Oxford University Press, New York, 1999).
[15] C. Hosokawa, H. Higashi, and T. Kusumoto, Appl. Phys. Lett. **62**, 3238 (1993).
[16] J. Cornil, D. Beljonne, and J. L. Brédas, J. Chem. Phys. **103**, 834 (1995).
[17] L. Torsi *et al.*, Science **272**, 1462 (1996).
[18] K. Waragai *et al.*, Phys. Rev. B **52**, 1786 (1995).
[19] S. Nelson *et al.*, Appl. Phys. Lett. **72**, 1854 (1998).
[20] L. Torsi *et al.*, Solid-State Electron. **45**, 1479 (2001).
[21] A. S. Davydov, *Theory of Molecular Excitons* (Plenum Press, New York, 1971).
[22] D. W. Schlosser and M. R. Philpott, Chem. Phys. **49**, 181 (1980).
[23] M. Oehzelt, R. Resel, and A. Nakayama, Phys. Rev. B **66**, 174104 (2002).
[24] K. Hummer, P. Puschnig, and C. Ambrosch-Draxl, Phys. Rev. B **67**, 184105 (2003).
[25] E. Sjöstedt, L. Nordström, and D. J. Singh, Solid State Commun. **114**, 15 (2000).
[26] P. Blaha *et al.*, in *WIEN2k, An Augmented Plane Wave + Local Orbitals Program for Calculating Crystal Properties* (Vienna University of Technology, Vienna, 2001).
[27] K. Hummer *et al.*, Synth. Met. **137**, 935 (2003).
[28] M. Rohlfing and S. G. Louie, Phys. Rev. Lett. **82**, 1959 (1999).
[29] L. Sham and T. Rice, Phys. Rev. **144**, 708 (1966).
[30] P. Puschnig and C. Ambrosch-Draxl, Phys. Rev. B **66**, 165105 (2002).
[31] K. Hummer, P. Puschnig, and C. Ambrosch-Draxl, Phys. Scr. (to be published).
[32] M. Kobayashi, K. Mizuno, and A. Matsui, J. Phys. Soc. Jpn. **58**, 809 (1989).
[33] We have verified this assignment by calculating the *c* components of the optical conductivity, the extinction coefficient, and the optical absorption coefficient.
[34] L. E. Lyons and G. C. Morris, J. Chem. Soc. 1551 (1959).
[35] S. Wiederhorn and H. G. Drickamer, J. Phys. Chem. Solids **9**, 330 (1959).
[36] R. Sonnenschein, K. Syassen, and A. Otto, J. Chem. Phys. **74**, 4315 (1981).
[37] L. Hedin, Phys. Rev. **139**, A796 (1965).
[38] G. Brocks, P. J. Kelly, and R. Car, Synth. Met. **57**, 4243 (1993).